Rashba-enhanced plasmon in a two-dimensional lateral superlattice

D. C. Marinescu and F. Lung
Department of Physics and Astronomy, Clemson University, Clemson, South Carolina 29634, USA
(Received 1 July 2010; revised manuscript received 18 October 2010; published 18 November 2010)

The self-consistent density response of an electron system is studied in a two-dimensional (2D) lateral superlattice (SL) with spin-orbit interaction (SOI). Under the effect of the lateral periodic potential, the single-electron 2D states are broadened into minibands that are spin split by SOI. In the case of a single fully occupied miniband, we calculate the long-wavelength limit of the polarization function for intraband transitions, within the random-phase approximation at $T=0$ K, and identify the plasmonic dispersion relation in the effective-mass approximation. The interplay between band effects and SOI coupling, considered here to be linear in the electron momentum (Rashba), is shown to generate a highly anisotropic collective excitation spectrum. If the plasmon propagating perpendicular on the superlattice axis has the characteristic frequency of the quasi-one-dimensional system weakly modified by the SOI split, the one propagating along the SL axis is enhanced by the SOI that couples, through its dependence on the periodic momentum of a Bloch electron, density fluctuations in different layers of the superlattice. The excitation frequency of this mode is found to depend on the miniband width and the amplitude of the SOI coupling constant.

DOI: 10.1103/PhysRevB.82.205322 PACS number(s): 71.45.Gm, 71.70.Ej, 73.21.Cd, 73.61.Ey

I. INTRODUCTION

The impact of the spin-orbit interaction (SOI) on various properties of electron systems has been a subject of great interest in the recent spintronics research.[1] The interaction, which appears as a result of the broken inversion symmetry in zinc-blende two-dimensional (2D) structures (Rashba) or in bulk (Dresselhaus),[2,3] determines a significant change in the single-particle energy spectrum with consequences on many static or dynamic properties. In this context, a great deal of attention was given to the SOI-induced modifications of the collective behavior of the electrons, especially to the polarization function that describes the density response to an applied electric potential and determines the screening through its participation in the dielectric function. Early analysis of the screening function in homogeneous 2D systems[4–6] indicated that in the presence of SOI, the long-wavelength limit of its poles, given by the real part of the polarization, and the corresponding plasmon frequencies are basically unchanged. This can be understood simply by recognizing that spin-symmetric, density-dependent properties are left invariant by the spin rotation caused by SOI while second-order effects are overshadowed by the usual plasmonic values. More significant is the impact of SOI on the many-body properties determined by the imaginary part of the polarization function, such as the electron relaxation rates[7,8] or from the plasmon decay into electron-hole pairs. The latter appears to exhibit unexpected features in the presence of both Rashba and Dresselhaus couplings, when it was found that along preferential directions in the electron-hole continuum (EHC), for certain values of the wave vector, the plasmons are overdamped, resulting in a filtering effect.[9]

In this paper, we extend the investigation of the real part of the polarization function to a 2D lateral superlattice (SL) with a Rasba-type spin-orbit coupling that is linear in the electron momentum.[10–13] This system is obtained by subjecting a 2D electron layer to an external periodic potential that localizes the electrons along certain spatial directions. When tunneling occurs between the quantum wires thus created, the single-electron states broaden into minibands whose width is proportional to the tunneling probability. Superlattice systems, in both two and three dimensions, have long been appreciated by theorists and experimentalists alike for the possibility of tailoring their properties in the growth process and thus obtain the most favorable situation for the observation of various phenomena.[14–17] Previous discussions of the collective excitation modes have underlined the sensitivity of the plasmonic excitation frequencies to band effects and the changes brought by periodicity on the Coulomb interaction. These characteristics are especially apparent in the dispersion relation of the plasmon mode propagating parallel to the superlattice axis, whose existence is a result of the coupling between density excitations in different wires intermediated by tunneling.[18–20] We anticipate therefore, that in the presence of SOI, the frequency of a plasmon that propagates along the symmetry axis of the SL will be strongly modified considering that electrons in different wires will now be coupled through the Rashba interaction that depends on the Bloch velocity of the electrons.

The real part of the polarization function is calculated self-consistently within the random-phase approximation (RPA) by following the equation-of-motion algorithm, previously used successfully to analyze response functions in two and three dimensional SLs.[14–17] In the long-wavelength limit the poles of the dielectric function are determined. The ensuing dispersion relations are found to be highly anisotropic. The plasmon that propagates along a direction perpendicular on the SL axis has a minimally lower frequency than the one in the absence of the SO coupling, similar to the case of homogeneous 2D systems. Quite differently, however, the collective excitation along the superlattice axis, in the case of a fully occupied miniband, is enhanced by existence of the Rashba interaction. Numerical results for two different SLs are discussed.

II. THEORETICAL MODEL

The system under consideration is obtained by subjecting a 2D electron layer to an additional attractive potential that is periodic along the $\hat{x}$ direction. The confining potential acts on a finite region of width b and has periodicity a. We will assume that $b \ll a$, but remains finite, such that the Coulomb interaction is that of a 2D system. A suitable choice of potential and b can be made, assuring that the energy difference between the ground-state level in the well and the next excited state is much larger than any of the broadening effects induced by tunneling and spin-orbit effects. Moreover, this approximation allows one to consider that in the presence of an electric potential, density excitations that occur within the lowest miniband are decoupled from other possible excitations and they constitute our present interest.[15–17] Tunneling occurs between the quasi-one-dimensional wires thus constructed and, as a result, the single-particle states inside the wells broaden into minibands that are spin spit by the SO interaction.

In the absence of SOI, the eigenstate of an electron of momentum $\mathbf{k}=\{k_x,k_y\}$, spin σ and effective mass m^* in the lateral superlattice is built as a Bloch function from the single-particle state inside the wire $\nu(x)$, multiplying an up- or down-spin state $\chi_\sigma=\{|\uparrow\rangle,|\downarrow\rangle\}$,

$$\psi_{k_x,k_y,\sigma}=\frac{1}{\sqrt{L_y}}e^{ik_y y}\xi_{k_x}(x)\chi_\sigma \tag{1}$$

with

$$\xi_{k_x}(x)=\frac{R_{k_x}}{\sqrt{N}}\sum_l e^{ik_x la}\nu(x-la). \tag{2}$$

k_x is subject to periodic boundary conditions, and is given by $k_x=\frac{2\pi}{Na}j$, where $j\in[-N/2,N/2]$. The normalization factor R_{k_x} differs from 1 by the overlap between states in two adjacent wells, $\gamma=\int_{-\infty}^{\infty}dx\nu(x)\nu(x-a)$,

$$R_{k_x}=[1+2\gamma\cos k_x a]^{-1/2}. \tag{3}$$

With $\Delta=4\int_{-b/2}^{b/2}dx\nu(x)V(x)\nu(x-a)$, the single-particle energy is written, in respect with the minimum of the band, as

$$\epsilon_{\mathbf{k}\sigma}=\frac{\hbar^2k_y^2}{2m}+\frac{\Delta}{2}(1-\cos k_x a). \tag{4}$$

When a Rasba-type interaction of coupling constant α is present, $H_R=\alpha(\sigma\times\mathbf{p})\hat{z}$, the spin-degenerate miniband splits. In a perturbative approach,[10,11] the energy spectrum is determined within the tight-binding approximation by performing a diagonalization of the Rashba interaction within the Hilbert space of the single-particle states, Eq. (1). The electron momenta that participate in the SO coupling are

$$p_y=\hbar k_y,$$

$$p_x=\frac{m^*}{\hbar}\frac{\partial\epsilon_{k_x,k_y,\sigma}}{\partial k_x}=\left(\frac{m^*a\Delta}{2\hbar}\right)\sin k_x a. \tag{5}$$

Two new chiral minibands corresponding to chiral quantum number $\mu=\pm1$ emerge, their associated single-particle energy being,

$$E_{\mathbf{k},\mu}=\epsilon_{\mathbf{k}}+\alpha\mu\sqrt{(\hbar k_y)^2+\left(\frac{m^*a\Delta}{2\hbar}\right)^2\sin^2 k_x a}. \tag{6}$$

The corresponding eigenstate is given by, $\psi_{\mathbf{k},\mu}(x,y)=e^{ik_y y}\xi_{k_x}(x)|\mu\rangle_{\mathbf{k}}$. The spinor $|\mu\rangle_{\mathbf{k}}$ represents a linear combination of up and down spin states whose coefficients are momentum dependent,

$$|\mu\rangle_{\mathbf{k}}=\frac{1}{\sqrt{2}}[|\uparrow\rangle+\mu e^{i\varphi_k}|\downarrow\rangle]. \tag{7}$$

The chiral angle φ_k is specified through its trigonometric functions,

$$\sin\varphi_k=\frac{p_y}{p}=\frac{\hbar k_y}{\sqrt{(\hbar k_y)^2+\left(\frac{m^*a\Delta}{2\hbar}\right)^2\sin^2 k_x a}},$$

$$\cos\varphi_k=\frac{p_x}{p}=\frac{\frac{m^*\Delta a}{\hbar}\sin k_x a}{\sqrt{(\hbar k_y)^2+\left(\frac{m^*a\Delta}{2\hbar}\right)^2\sin^2 k_x a}}, \tag{8}$$

where $p=\sqrt{p_x^2+p_y^2}$ is the magnitude of the electron momentum.

The limits of this approximation were tested in Ref. 21. There the electron Bloch functions in the superlattice were constructed from the single-particle eigenstates of the Rashba Hamiltonian in each wire, the spin coefficients and the single-particle energies being calculated in the tight-binding approximation. The dispersion relations for the lowest-two chiral minibands found in this way are similar to those expressed in Eq. (6). Moreover, the points of chiral-spin degeneracy, at $k_x=0,\pm\pi/a$ are preserved. Since the physical properties discussed in this paper are obtained through an algorithm that integrates over all the energy states within the two lowest-lying minibands, the analytic model presented above is expected to provide an adequate qualitative and quantitative description of the problem for a large range of values of Δ and α.

III. DENSITY RESPONSE FUNCTION

We calculate the self-consistent density response function to an electric field within the RPA by following the equation-of-motion method.[14,22,23] The particle density fluctuations induced by a perturbation are expressed as the difference between the average of the density operator on the unperturbed ground state, denoted by $\langle\cdots\rangle_0$, and the equilibrium density,

$$n(\mathbf{r},t) = \langle \Psi^{\dagger}(\mathbf{r},t)\Psi(\mathbf{r},t)\rangle_0 - n^0. \tag{9}$$

The field operator $\Psi(\mathbf{r},t)$ is a linear combination of single-particle states $\psi_{\mathbf{k}}(x,y)$ multiplying destruction (creation) operators $c^{(\dagger)}_{\mathbf{k},\mu}(t)$,

$$\Psi(\mathbf{r},t) = \sum_{\mathbf{k},\mu} \psi_{\mathbf{k}}(x,y) c_{\mathbf{k},\mu}(t). \tag{10}$$

$\langle \cdots \rangle_0$ in Eq. (9) denotes the average on the unperturbed ground state. The Fourier transform of the time-dependent density fluctuation is given by,

$$n(\mathbf{q},t) = \sum_{\mathbf{k}\mu,\mathbf{k}'\mu'} \langle \mathbf{k}\mu | e^{-i\mathbf{q}\cdot\mathbf{r}} | \mathbf{k}'\nu\rangle \langle c^{\dagger}_{\mathbf{k},\mu}(t) c_{\mathbf{k}',\nu}(t)\rangle_0 - n^0 \delta_{\mathbf{q},0}. \tag{11}$$

An electric potential $-e\upsilon(\mathbf{r})$ generates the interaction Hamiltonian

$$H_{int} = -e\int d\mathbf{r}\upsilon(\mathbf{r}) n(\mathbf{r},t) = \sum_{\mathbf{k}\mu,\mathbf{k}'\nu} \langle \mathbf{k}\mu | \upsilon(\mathbf{r}) | \mathbf{k}'\nu\rangle c^{\dagger}_{\mathbf{k},\mu}(t) c_{\mathbf{k}',\mu}(t) \tag{12}$$

which determines the time evolution of the density fluctuations through the equation of motion,

$$i\hbar \left\langle \frac{\partial n}{\partial t} \right\rangle_0 = \langle [H, n(t)]\rangle_0. \tag{13}$$

The result of this algorithm is expressed in terms of the frequency- and wave-vector-dependent density fluctuation $n(\mathbf{q},\omega)$,

$$n(\mathbf{q},\omega) = \sum_{\mathbf{k}\mu;\mathbf{k}'\nu} \frac{n^0_{\mathbf{k},\mu} - n^0_{\mathbf{k}',\nu}}{E_{\mathbf{k},\mu} - E_{\mathbf{k}',\nu} + \hbar\omega} \langle \mathbf{k}\mu | e^{-i\mathbf{q}\cdot\mathbf{r}} | \mathbf{k}'\nu\rangle \times \langle \mathbf{k}'\nu | (-e\upsilon) | \mathbf{k}\mu\rangle. \tag{14}$$

$n^0_{\mathbf{k},\mu} = \langle c^{\dagger}_{\mathbf{k}\mu} c^{\dagger}_{\mathbf{k}\mu}\rangle_0$ represents the equilibrium occupation number for a given single-particle state $|\mathbf{k},\mu\rangle$ of energy $E_{\mathbf{k},\mu}$. Within the RPA, the electric potential $-e\upsilon(\mathbf{r})$ is self-consistently induced by the fluctuations.

$$-e\upsilon(\mathbf{r}) = \int d\mathbf{r}' \frac{e^2}{|\mathbf{r}-\mathbf{r}'|} n(\mathbf{r}',t) = \sum_{\mathbf{q}_0} \upsilon(q_0) e^{i\mathbf{q}_0\cdot\mathbf{r}} n(\mathbf{q}_0,t), \tag{15}$$

where $\upsilon(q_0) = 2\pi e^2/\varepsilon q_0$ is the Fourier transform of the Coulomb interaction in a 2D system of dielectric constant ε. The matrix element of the self-consistent potential between the states labeled by $\{\mathbf{k}\mu\}$ and $\{\mathbf{k}'\nu\}$ is

$$\langle \mathbf{k}'\nu | -e\upsilon(\mathbf{r}) | \mathbf{k}\mu\rangle = -e\sum_{\mathbf{q}_0} \upsilon(q_0) \langle \mathbf{k}'\nu | e^{i\mathbf{q}_0\cdot\mathbf{r}} | \mathbf{k}\mu\rangle n(\mathbf{q}_0,\omega). \tag{16}$$

Equations (14)–(16), provide the self-consistent equation satisfied by the particle fluctuations in the RPA,

$$n(\mathbf{q},\omega) = \sum_{\mathbf{k}\mu;\mathbf{k}'\nu} \frac{n^0_{\mathbf{k},\mu} - n^0_{\mathbf{k}'\nu}}{E_{\mathbf{k},\mu} - E_{\mathbf{k}',\nu} + \hbar\omega} \langle \mathbf{k}\mu | e^{-i\mathbf{q}\cdot\mathbf{r}} | \mathbf{k}'\nu\rangle \times \sum_{\mathbf{q}_0} \upsilon(q_0) \langle \mathbf{k}'\nu | e^{i\mathbf{q}_0\cdot\mathbf{r}} | \mathbf{k}\mu\rangle n(\mathbf{q}_0,\omega) \tag{17}$$

For a given pair of states $\{\mathbf{k}\mu\},\{\mathbf{k}',\nu\}$, the simultaneous existence of the two matrix elements, $\langle \mathbf{k}\mu | e^{-i\mathbf{q}\cdot\mathbf{r}} | \mathbf{k}'\nu\rangle$ and $\langle \mathbf{k}'\nu | e^{i\mathbf{q}_0\cdot\mathbf{r}} | \mathbf{k}\mu\rangle$, implies, $\mathbf{q} = \mathbf{q}_0$.[23] Hence,

$$n(\mathbf{q},\omega) = \sum_{\mathbf{k}\mu;\mathbf{k}'\nu} \frac{n^0_{\mathbf{k},\mu} - n^0_{\mathbf{k}',\nu}}{E_{\mathbf{k},\mu} - E_{\mathbf{k}',\nu} + \hbar\omega} \times |\langle \mathbf{k}\mu | e^{-i\mathbf{q}\cdot\mathbf{r}} | \mathbf{k}'\nu\rangle|^2 \upsilon(q) n(\mathbf{q},\omega). \tag{18}$$

The matrix element that appears in the above expression is calculated explicitly when the components of $\mathbf{k} = \{k_x, k_y\}$ are introduced. We obtain,

$$\langle k_x, k_y, \mu | e^{-i\mathbf{q}\cdot\mathbf{r}} | k'_x, k'_y, \nu\rangle = \langle k'_x | e^{-iq_x x} | k_x\rangle \times \langle k'_y | e^{-iq_y y} | k_y\rangle F_{\mu\nu}(k_x, k_y, k'_x, k'_y). \tag{19}$$

The chiral form factor $F_{\mu\nu}(k_x, k_y, k'_x, k'_y)$ is produced by the overlap of the two spinors $|\mu\rangle_{\mathbf{k}}$ and $|\nu\rangle_{\mathbf{k}'}$ in the spin space, Eq. (7),

$$F_{\mu\nu}(k_x, k_y, k'_x, k'_y) = {}_{\mathbf{k}}\langle \mu | \nu\rangle_{\mathbf{k}'} = \frac{1}{2}[1 + \mu\nu e^{-i\varphi_{\mathbf{k}} + i\varphi_{\mathbf{k}'}}]. \tag{20}$$

The orthogonality of the single-particle states imposes the conservation of the momentum $\mathbf{k}' = \mathbf{k} + \mathbf{q}$, which implies, $\langle k_y | e^{-iq_y y} | k'_y\rangle = \delta_{k'_y, k_y + q_y}$ and $\langle k_x | e^{-iq_x x} | k' x\rangle = \delta_{k'_x, k_x + q_x} A(k_x, k_x + q_x)$, where $A(k_x, q_x)$ results from the overlap of the single-electron states, Eq. (2), along the $\hat{x}$ direction,

$$A(k_x, q_x + k_x) = R_{k_x} R_{k_x + q_x} \sum_l e^{-ik_x la} \int_{-\infty}^{\infty} dx \nu(x) e^{-iq_x x} \nu(x - la). \tag{21}$$

In the tight-binding approximation, $A(k_x, q_x + k_x)$ can be calculated to be

$$A(k_x, q_x) = R_{k_x} R_{k'_x} \left\{ \int_{-\infty}^{\infty} dx \nu(x)^2 e^{iq_x x} + 2\,\Re e\left[e^{ik_x a} \int_{-\infty}^{\infty} dx \nu(x) e^{iq_x a} \nu(x - a) \right] \right\}. \tag{22}$$

($\Re e$ denotes the real part of a complex number.)

Because of the superlattice periodicity along the $\hat{x}$ direction, the momentum transfer q_x can be defined only up to a reciprocal-lattice vector $2\pi s/a$ when umklapp processes are included. Therefore, if $\mathbf{q}$ is restricted to reside in the first Brillouin zone, the self-consistent equation satisfied by the intraband density fluctuations is obtained, with input from Eqs. (18)–(21) written for $q_x \to q_x + 2\pi s/a$, to be,

$$n(\mathbf{q},\omega)\Bigg[1-\sum_{\mu\nu}\sum_{k_x,k_y}\frac{n^0_{\mathbf{k}-\mathbf{q}/2,\mu}-n^0_{\mathbf{k}+\mathbf{q}/2,\nu}}{E_{\mathbf{k}-\mathbf{q}/2,\mu}-E_{\mathbf{k}+\mathbf{q}/2,\mu}+\hbar\omega}\times|F_{\mu\nu}(k_x,k_y,q_x,q_y)|^2\sum_s\frac{2\pi e^2|A(k_x,q_x+2\pi s/a)|^2}{\sqrt{(q_x+2\pi s/a)^2+q_y^2}}\Bigg]=0. \tag{23}$$

This final form takes advantage of the fact that with the exception of the longitudinal form factor A and the Coulomb interaction Fourier transform, $v(q)$, all the functions are periodic in the reciprocal space and are left invariant by umklapp scattering.

IV. RESULTS AND CONCLUSIONS

The result of Eq. (23) is characteristic for single-miniband superlattices previously discussed in Refs. 14–17. An exact analytic estimate of its solutions for all values of frequency and wave vector is difficult considering the complicated expression of the single-particle energy. An important simplification occurs in the weak tunneling regime, where only nearest-neighbor tunneling is considered. Then, in first order in the tunneling probability, the form factor $A(k_x,q_x)$ in Eq. (21) is independent of k_x regardless of the exact analytic form of the single well function $\nu(x)$.[15–17] This approximation allow the factorization of the double sum in Eq. (23) and enable the direct definition of the total polarization of the 2D lateral superlattice,

$$P(q_x,q_y,\omega)=\sum_{k_x\mu,k_y\nu}\frac{n^0_{\mathbf{k}-\mathbf{q}/2,\mu}-n^0_{\mathbf{k}+\mathbf{q}/2,\nu}}{E_{\mathbf{k}-\mathbf{q}/2,\mu}-E_{\mathbf{k}+\mathbf{q}/2,\mu}+\hbar\omega}\times|F_{\mu\nu}(k_x,k_y,q_x,q_y)|^2, \tag{24}$$

where, from Eq. (20),

$$|F_{\mu\nu}(\mathbf{k},\mathbf{q})|^2=\frac{1}{2}[1+\mu\nu\cos(\varphi_{\mathbf{k}-\mathbf{q}/2}-\varphi_{\mathbf{k}+\mathbf{q}/2})]. \tag{25}$$

The structure of Eq. (24) is that of the usual real part of the polarization function of a 2D free-electron system with SOI,[4] except for the different dispersion of the single-particle energies.

The symmetry of the chiral form factors and of the single-particle energies that are even functions of $\mathbf{k}$, permits a rearrangement of the terms in Eq. (24),

$$P(\mathbf{q},\omega)=\sum_{\mathbf{k},\mu}n^0_{k,\mu}\Bigg[\frac{2(E_{\mathbf{k}+\mathbf{q},\mu}-E_{\mathbf{k},\mu})|F_{\mu\mu}(\mathbf{k}+\mathbf{q}/2,\mathbf{q})|^2}{(\hbar\omega)^2-(E_{\mathbf{k}+\mathbf{q},\mu}-E_{\mathbf{k},\mu})^2}+\frac{2(E_{\mathbf{k}+\mathbf{q},-\mu}-E_{\mathbf{k},\mu})|F_{\mu,-\mu}(\mathbf{k}+\mathbf{q}/2,\mathbf{q})|^2}{(\hbar\omega)^2-(E_{\mathbf{k}+\mathbf{q},-\mu}-E_{\mathbf{k},\mu})^2}\Bigg]. \tag{26}$$

In the plasmon frequency domain, the contribution to the overall value of the polarization function comes only from the intrachiral fluctuations ($\mu=\nu$) and it is customary to consider that in the corresponding denominators $\hbar\omega\gg\Delta E$. The intrachiral excitations ($\mu\neq\nu$) are realized only for values of the frequency above a certain finite threshold and do not participate to the long-wavelength ($q\to0$) oscillations. Thus, if we expand in terms of the ratio $\Delta E/\hbar\omega$, and then in a power series, up to second order, in $\mathbf{q}$, we obtain the long-wave-vector polarization expression,

$$P(\mathbf{q},\omega)=\frac{1}{(\hbar\omega)^2}\sum_{\mu,k_x,k_y}n^0_{\mathbf{k},\mu}\Bigg[\left(q_x^2\frac{\partial^2}{\partial k_x^2}+q_y^2\frac{\partial^2}{\partial k_y^2}\right)E_{\mathbf{k},\mu}\Bigg]. \tag{27}$$

Equation (27) represents the effective mass approximation of the polarization function since the second-order derivatives of the energy are proportional to the effective masses along the corresponding directions.[18–20] The energy dispersions, Eq. (6), generate two highly anisotropic results

$$\frac{\partial^2E_{\mathbf{k},\mu}}{\partial k_x^2}=\frac{\Delta a^2}{2}\cos k_xa+\alpha\mu\Bigg[\frac{p_y^2}{p^3}\left(\frac{dp_x}{dk_x}\right)^2+\frac{p_x}{p}\frac{d^2p_x}{dk_x^2}\Bigg], \tag{28}$$

$$\frac{\partial^2E_{\mathbf{k},\mu}}{\partial k_y^2}=\frac{\hbar^2}{2m^*}+\alpha\mu\frac{p_x^2}{p^3}\left(\frac{dp_y}{dk_y}\right)^2. \tag{29}$$

It is apparent at this point that the distinct dispersion of the plasmonic mode propagating parallel to the SL axis is the periodicity of the velocity of a Bloch electron that participates in the SOI coupling, for which $p_xd^2p_x/dk_x^2<0$ in Eq. (28). This term originates in the interplay between tunneling effects that determine the bandwidth and the Rashba interaction which determines the velocity-dependent energy spectrum. Since its sign is always negative, it provides a counterbalance to the first term in Eq. (28) that changes the overall contribution of the Rashba interaction to the plasmon frequency.

The analytic estimate of Eq. (27) requires several input considerations. First, the two minibands of opposite chirality are assumed to be fully occupied, setting the maximum value of the x-axis momentum, $k_{F_x\mu}=\pi/a$. For a given total particle density n, and implicitly a set Fermi energy E_F, the maximum value of the momentum p_y is determined by the solutions of $E_F=E_{k_x,p_{Fy},\mu}$ for each value of k_x. With p_x and p_y from Eq. (5), the Fermi momenta along the y axis, as functions of k_x, are calculated to be

$$p_{F_y\mu}(k_xa)=\sqrt{2m^*\Bigg[E_F-\Delta\sin^2\frac{k_xa}{2}+m^*\alpha^2-\alpha\mu\sqrt{2m\left(E_F-\Delta\sin^2\frac{k_xa}{2}\right)+p_x^2+m^{*2}\alpha^2}\Bigg]}. \tag{30}$$

The existence of both solutions for all values of k_x requires that the Fermi energy satisfies $E_F > \Delta(1+\alpha m a/\hbar)$. This condition constrains the relationship between the independent parameters of the problem, Δ, α, and a.

At $T=0$ K, the particle occupation number is represented by the product of two independent Heaveside functions, $n^0_{\mathbf{k},\mu} = \theta(\frac{\pi}{a} - |k_x|)\,\theta(k_{F_{y\mu}} - |k_y|)$ which allow the factorization of the sum over $\mathbf{k}$. The connection between the particle density n and the Fermi energy is therefore given by,

$$n = \frac{1}{\pi^2 a\hbar}\int_0^\pi d(k_x a)[p_{F_{y+}}(k_x a) + p_{F_{y-}}(k_x a)], \tag{31}$$

where the evenness of the integration kernel was considered. Equation (31) has to be satisfied consistently with the condition on E_F that guarantees the existence of the two Fermi momenta.

The same computational algorithm is used estimating Eq. (27) which becomes,

$$\begin{aligned} P(\mathbf{q},\omega) = {} & \frac{1}{\pi^2\hbar a(\hbar\omega)^2}\frac{\Delta a^2}{2}\int_0^\pi d(k_x a)\Bigg\{(p_{F_{y+}} + p_{F_{y-}})\cos(k_x a) \\ & + \frac{m^*\alpha a}{\hbar}\left(\frac{m^*\Delta a}{2\hbar}\right)\Bigg[\left(\frac{p_{F_{y-}}}{\sqrt{p^2_{F_{y-}} + p_x^2}} \right. \\ & \left. - \frac{p_{F_{y+}}}{\sqrt{p^2_{F_{y+}} + p_x^2}}\right)\cos^2(k_x a) \\ & - \cos(2k_x a)\ln\left(\frac{p_{F_{y-}} + \sqrt{p^2_{F_{y-}} + p_x^2}}{p_{F_{y+}} + \sqrt{p^2_{F_{y+}} + p_x^2}}\right)\Bigg]\Bigg\} q_x^2 \\ & + \frac{n q_y^2}{\omega^2 m^*}\left[1 - \frac{m^*\alpha}{n\pi^2\hbar a}\int_0^\pi d(k_x a)(p_{F_{y-}} - p_{F_{y+}})\right], \end{aligned} \tag{32}$$

where Eqs. (28) and (29) were employed. The insertion of Eq. (32) in Eq. (23), generates the final form of the dispersion law,

$$\begin{aligned} \omega^2 = {} & \frac{e^2\Delta}{\varepsilon m^*\pi\hbar^3}\int_0^\pi d(k_x a)\Bigg\{(p_{F_{y+}} + p_{F_{y-}})\cos k_x a \\ & + \frac{m^*\alpha a}{\hbar}\left(\frac{m^*\Delta a}{2\hbar}\right)\Bigg[\left(\frac{p_{F_{y-}}}{\sqrt{p^2_{F_{y-}} + p_x^2}} \right. \\ & \left. - \frac{p_{F_{y+}}}{\sqrt{p^2_{F_{y+}} + p_x^2}}\right)\cos^2(k_x a) \\ & - \cos(2k_x a)\ln\left(\frac{p_{F_{y-}} + \sqrt{p^2_{F_{y+}} + p_x^2}}{p_{F_{y+}} + \sqrt{p^2_{F_{y+}} + p_x^2}}\right)\Bigg](aq_x)^2 + \frac{2\pi n e^2}{\varepsilon m^*} \\ & \times\left[1 - \frac{m^*\alpha}{n\pi^2\hbar a}\int_0^\pi d(k_x a)(p_{F_{y-}} - p_{F_{y+}})\right](aq_y)^2\Bigg\} \\ & \times\sum_s \frac{|A(aq_x + 2\pi s)|^2}{\sqrt{(aq_x + 2\pi s)^2 + (aq_y)^2}}. \end{aligned} \tag{33}$$

Equation (33) reproduces the usual result obtained in homogeneous 2D lateral superlattice for the propagation along the y direction,[17,20] modified by the presence of SOI coupling. Along the x direction the dispersion shows proportionality with the miniband width Δ and an enhancement proportional with the Rashba coupling constant whose existence originates in the periodicity of the Bloch velocity that assures the coupling between the density fluctuations in the different SL wires that oscillate in phase. In the following considerations, we focus on the Eq. (33) written for $q_y=0$.

The free propagation of the x plasmon is limited by the presence of the EHC, the region in the ω-q plane that corresponds to the creation of electron-hole pairs. The limits of the EHC are given by equations that describe the maximum value of the energy difference for a momentum transfer of magnitude q, $\hbar\omega = |E_{\mathbf{k}+\mathbf{q},\mu} - E_{\mathbf{k},\nu}|$, for states on the Fermi surface. Accordingly, for $q_y=0$, intrachiral transitions are limited by

$$\begin{aligned} & \hbar\omega^{-+}(q_x, q_y = 0) \\ & = \frac{\Delta}{2}\sin^2\frac{q_x a}{2} + \alpha\sqrt{p^2_{F-}(\pi/a + q_x) + p_x^2(\pi/a + q_x)} \\ & \quad + \alpha p_{F-}(\pi/a), \\ & \hbar\omega^{+-}(q_x, q_y = 0) \\ & = -\frac{\Delta}{2}\sin^2\frac{q_x a}{2} + \alpha\sqrt{p^2_{F-}(\pi/a + q_x) + p_x^2(\pi/a + q_x)} \\ & \quad + \alpha p_{F+}(\pi/a) \end{aligned} \tag{34}$$

while the electron-hole continuum boundary for the intrachiral modes is established by

$$\begin{aligned} & \hbar\omega^{--}(q_x, q_y = 0) \\ & = \frac{\Delta}{2}\sin^2\frac{q_x a}{2} + \alpha\sqrt{p^2_{F-}(\pi/a + q_x) + p_x^2(\pi/a + q_x)} - \alpha p_{F-}. \end{aligned} \tag{35}$$

Free propagation occurs in the range $\omega^{--} < \omega < \omega^{+-}$.

To illustrate our results, we choose two distinct configurations comparable to experimentally studied samples of GaAs lateral superlattices. The material parameters are $\hbar\alpha = 5\times10^{-11}$ eV m,[24] $m^* = 0.067 m_0$, $\varepsilon = 13.0$. The periodic confining potential is assumed to be parabolic, of strength $(m^*/2)(\Delta/\hbar)^2 x^2$, leading to a longitudinal form factor in Eq. (22), $A(q_x) = e^{-(\hbar q_x)^2/4m^*\Delta}$. A quick inspection of Eq. (33) indicates that the values of the remaining SL parameters n, a, Δ determine a great range of possible values for the outcome. Our parameter selection is done such that the effect of the Rashba interaction is maximized.

In the first case, we consider a superlattice whose miniband width Δ is comparable with the Rashba interaction. For SL parameters $a = 38$ nm, $\Delta = 11$ meV, and $n = 2.6\times10^{15}$ m^{-2} the Fermi energy is obtained to be $E_F = 21$ meV. The calculated Rashba interaction is about 10.5

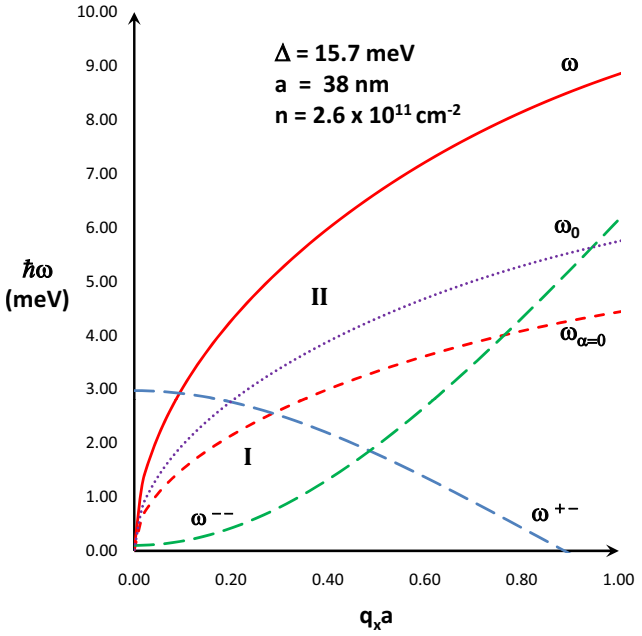

FIG. 1. (Color online) The frequency of x-axis plasmon propagating in a lateral superlattice whose bandwidth Δ is comparable with the Rashba coupling is plotted as a function of $q_x a$. The SL parameters are $\Delta=11$ meV, $a=38$ nm, and $n=2.6\times10^{15}$ m^{-2}. The increase in the frequency is approximately 40%. By comparison, plots of the excitation frequency in the absence of the SOI coupling $\omega_{\alpha=0}$ and the 2D isotropic plasmon mode in the presence of SOI are also represented in dotted lines. Free propagation occurs in region I.

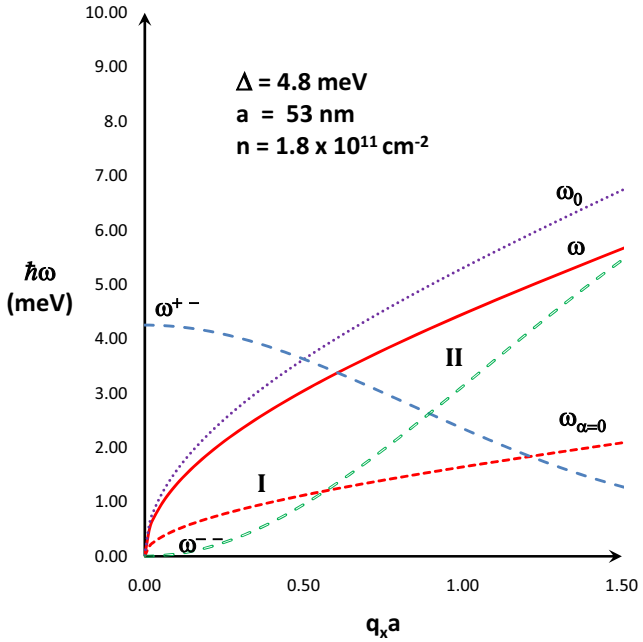

FIG. 2. (Color online) The frequency of x-axis plasmon propagating in a lateral superlattice whose bandwidth Δ is smaller the Rashba coupling is plotted as a function of $q_x a$. For $\Delta=4.8$ meV, $a=53$ nm, and $n=1.8\times10^{11}$ cm^{-2}, the Rashba coupling strength is 8 meV. For these parameters the increase in the frequency is approximately 66%. By comparison, plots of the excitation frequency in the absence of the SOI coupling $\omega_{\alpha=0}$ and the 2D isotropic plasmon mode in the presence of SOI ω_0 are also represented in dotted lines. Free propagation occurs in region I.

meV. The energy $\hbar\omega$ of the x-axis plasmon is plotted in Fig. 1 as a function of $q_x a$ for $q_y=0$, along with the EHC limits $\hbar\omega^{+-}$ and $\hbar\omega^{--}$ and the plasmon energy in the absence of the Rashba coupling, $\hbar\omega_{\alpha=0}$. A dotted line represents $\hbar\omega_0$, the frequency of the plasmon propagating in a 2D isotropic environment with SOI at the same density. The enhancement of the plasmon frequency generated by the Rashba coupling is about 40%. The plasmon propagates freely outside the EHC limits at small values of $q_x a$, in region I and is damped in region II, inside the EHC .

In Fig. 2, we plot the plasmon frequency for a SL whose bandwidth Δ is smaller than the maximum level of the Rashba interaction. For $a=53$ nm, $\Delta=4.8$ meV, and $n=1.8\times10^{11}$ cm^{-2}, the Fermi energy is calculated to be 16 meV, while the maximum Rashba interaction is approximately 8 meV. In this case, the Rashba determined enhancement of the plasmon frequency is even more pronounced, about 66%. While we acknowledge the simplicity of the model discussed above, we expect that the modified excitation frequency of the Rashba plasmon discussed here is directly experimentally observable and provide a measurable account of the SOI effect on the density-dependent properties of a 2D system. Moreover, the discrepancies between experiments and the theoretical prediction can serve as a guidance to understand the energy spectrum of the electrons in the SL.

ACKNOWLEDGMENTS

We gratefully acknowledge support in performing this work from DOE, Grant No. DE-FG02-04ER46139.

[1] I. Žutić, J. Fabian, and S. Das Sarma, Rev. Mod. Phys. **76**, 323 (2004).
[2] Y. Bychkov and E. I. Rashba, JETP Lett. **39**, 78 (1984).
[3] G. Dresselhaus, Phys. Rev. **100**, 580 (1955).
[4] M. Pletyukhov and V. Gritsev, Phys. Rev. B **74**, 045307 (2006).
[5] X. F. Wang, Phys. Rev. B **72**, 085317 (2005).
[6] M. S. Kushwaha and S. E. Ulloa, Phys. Rev. B **73**, 205306 (2006).
[7] I. A. Nechaev, I. Y. Sklyadneva, V. M. Silkin, P. M. Echenique, and E. V. Chulkov, Phys. Rev. B **78**, 085113 (2008).
[8] I. A. Nechaev, P. M. Echenique, and E. V. Chulkov, Phys. Rev. B **81**, 195112 (2010).
[9] S. M. Badalyan, A. Matos-Abiague, G. Vignale, and J. Fabian, Phys. Rev. B **79**, 205305 (2009).
[10] M. Governale and U. Zülicke, Phys. Rev. B **66**, 073311 (2002).
[11] P. Kleinert, V. V. Bryksin, and O. Bleibaum, Phys. Rev. B **72**, 195311 (2005).
[12] I. Vurgaftman and J. R. Meyer, Phys. Rev. B **70**, 205319 (2004).

[13] D. V. Khomitsky, Phys. Rev. B **77**, 113313 (2008).
[14] A. C. Tselis and J. J. Quinn, Phys. Rev. B **29**, 3318 (1984).
[15] S. Das Sarma and J. J. Quinn, Phys. Rev. B **25**, 7603 (1982).
[16] S. Das Sarma and W.-y. Lai, Phys. Rev. B **32**, 1401 (1985).
[17] W.-m. Que and G. Kirczenow, Phys. Rev. B **37**, 7153 (1988).
[18] D. Grecu, Phys. Rev. B **8**, 1958 (1973).
[19] X. Zhu, X. Xia, J. J. Quinn, and P. Hawrylak, Phys. Rev. B **38**, 5617 (1988).
[20] W.-m. Que and G. Kirczenow, Phys. Rev. B **36**, 6596 (1987).
[21] V. Demikhovskii and D. Khomitsky, JETP Lett. **83**, 340 (2006).
[22] H. Ehrenreich and M. H. Cohen, Phys. Rev. **115**, 786 (1959).
[23] X. Zhu and A. W. Overhauser, Phys. Rev. B **30**, 3158 (1984).
[24] S. D. Ganichev, V. V. Bel'kov, L. E. Golub, E. L. Ivchenko, P. Schneider, S. Giglberger, J. Eroms, J. De Boeck, G. Borghs, W. Wegscheider, D. Weiss, and W. Prettl, Phys. Rev. Lett. **92**, 256601 (2004).